Analysis of Polyaddition Levels in *i*-Sc_3NC_{80}

Josep M. Campanera,*,† Malcolm I. Heggie,‡ and Roger Taylor*,‡

Departament de Química Física i Inorgànica, Universitat Rovira i Virgili, 43005 Tarragona, Catalonia, Spain, and Chemistry Department, University of Sussex, Brighton BN1 9QJ, U.K.

Received: August 17, 2004

Using the density functional method, the stabilities of highly hydrogenated and fluorinated [80]fullerenes, both empty and containing the Sc_3N molecule, have been calculated. Addition of 44 atoms to *i*-Sc_3NC_{80} is predicted to be most favorable due to the formation of six octahedrally located benzenoid rings, while addition of up to 52 atoms (consistent with preliminary fluorination data) gives a structure stabilized by the presence of four benzenoid rings. The most stable isomers at this addition level have been determined and the relative stabilities of a number of $C_{80}H_{52}$, $C_{80}F_{52}$, and *i*-$Sc_3NC_{80}H_{52}$ species calculated. The hydrogenation of the *i*-Sc_3NC_{80} has been computed to be more difficult than the corresponding partner, C_{80}. From the geometrical point of view, the Sc_3N molecule is planar in the parent [80]fullerene but is calculated to be pyramidal in some of the hydrogenated/fluorinated derivatives. Moreover, in these it has fixed locations due to orbital interactions arising from deformation of the cage and the presence of localized double bonds.

1. Introduction

Fullerenes containing trimetallonitride groups (NM_3, M = rare earths and Group III metals) within the cage are a particularly interesting class of *incar*fullerenes (loosely termed *endohedral* fullerenes). Not only are the cage properties modified by the presence of the incarcerated group, but almost uniquely among *incar*fullerenes, they are quite stable. Moreover, they can be produced in multimilligram quantities, and these amounts should increase in future. The electronic effect of the trimetallonitride group is such that some fullerenes of sizes and symmetry that are otherwise relatively unstable become available for investigation. Thus far the following compounds have been structurally characterized: *i*-$Sc_3NC_{68}(D_3)$,[1] *i*-$Sc_3NC_{78}(D_{3h})$,[2] *i*-$ErSc_2C_{80}(I_h)$,[3] *i*-$Sc_3NC_{80}(I_h$ and $D_{5h})$,[4,5] and *i*-$Lu_3NC_{80}(I_h)$.[6]

The transfer of up to six electrons to fullerene cages, e.g. [60]-, [I_h-80]-, [D_2-84]- and [D_{2d}-84]fullerenes, greatly stabilizes them,[7] and theoretical calculations of the stabilities, geometries, and electronic structures of some trimetallonitride fullerenes have been made.[8,9]

The electron affinities of *i*-$Sc_nEr_{3-n}NC_{80}$ compounds have been investigated, though with inconclusive results.[10] In the case of incarcerated single atoms, it might be supposed that electron transfer from the metallic group to the cage surface would result in a decrease in electron affinity. However, the surface charge is delocalized over the whole cage and thus is ineffective in shielding the internal charge, so that an *increase* in electron affinity may be expected. The situation thus parallels the origins of electronegativity differences of the elements—the additional 'delocalized' orbiting electron does not fully shield the increased charge on the nucleus. In the case of *i*-Sc_3NC_{80}, evidence from comparison of HPLC retention times with those of empty fullerenes suggested that electron withdrawal by the nitrogen atom may decreases the electron density of the surface;[11] this should make radical addition (and cycloadditions) less favorable.

The chemistry of the trimetallonitride fullerenes may become a substantial area of fullerene research and is particularly interesting not only because of the electronic effect of the incarcerated molecule, but because unusual C−C bonding characteristics may exist on the cage surface. Thus, for example, I_h-C_{80} itself contains no high electron density π-bonds in contrast to the common fullerenes, so that cycloaddition could be expected to be difficult. Nevertheless [2 + 4] addition of 6,7-dimethoxyisochroman-3-one with *i*-Sc_3NC_{80} has been observed, the product structure being single-crystal X-ray characterized.[12] In this derivative, addition takes place across a 6:5 C−C bond rather than a 6:6 C−C bond, which we propose is due to the lower pentagon angle strain resulting from the former addition compared to the latter. The formation of water-soluble fullerenols *i*-$Sc_3NC_{80}(OH)_nO_n$ (n = ca. 10) has also been reported[13] (the value of n is very approximate as no structural characterization was obtained).

Preliminary data for hydrogenation of a very small quantity (ca. 1 mg) of *i*-Sc_3NC_{80} (mainly I_h but containing ca. 10% of the D_{5h} isomer) showed in two separate samples, the addition of 60H and 68H.[14] Subsequent investigation of fluorination of *i*-Sc_3NC_{80} using a larger sample gave a number of products that contained, in varying relative concentrations, between 42 and 64 fluorines. Because of the larger sample used, we consider that the fluorination results are the more reliable, and in all the fluorinated fractions *i*-$Sc_3NC_{80}F_{52}$ was present, being the dominant species in a number of them.[15] Because of the presence of the minor isomer (which is less soluble in toluene than the main one) and possibly others, we believe that further and meaningful experimental investigations of polyaddition can only be undertaken with larger quantities of the pure isomers, should these become available.

We have therefore carried out theoretical calculations to predict stabilities of derivatives of various addition levels, and to consider the stabilities in particular of various isomers at the X_{52} (X = H, F) addition level, first with and then without incarcerated Sc_3N. Although I_h C_{80} has yet to be isolated (cf. the D_2 and D_{5d} isomers[16,17]), it was necessary to work initially

* To whom correspondence should be addressed.
† Universitat Rovira i Virgili.
‡ University of Sussex.

10.1021/jp040557r CCC: $30.25
Published on Web 02/09/2005

TABLE 1: Hydrogenation Binding Energies (HBE/*n*, eV) per Added H_2 of the Most Stable $C_{80}H_x$ and *i*-$Sc_3NC_{80}H_x$ Isomers[a]

x	H atom locations [a]	benzenoid rings[b]	C=C bonds[b]	sym[c]	HBE/n for $C_{80}H_x$[d]	HBE/n for *i*-$Sc_3NC_{80}H_x$[e]
2	1,2	0	−	C_s	−1.25	−
4	1,2,7,23	0	−	C_{2v}	−1.24	−
16	3−8, 25−31,13−15	A	−	C_{2v}	−1.04	−
36	*f*	A,C,D	−	C_2	−1.05	−
44	−	A,B,C,D,E,F	−	T_h	−1.08	−0.64
48	−	A,B,C,D	18,19;37,38, 58,59;61,75	C_s	−0.92	−0.53
52:**1**	−	A,B,C,D	23,24;32,33	C_{2v}	−0.83	−0.47
52:**5**	−	A,B,C,D	22,23;33,34	C_s	−0.82	−0.49
72	−	0	1,2;39,40;41,60; 78,79	C_s	−0.35	−0.10
76	−	0	1,2;78,79	C_s	−0.20	−
78	−	0	1,2	C_s	−0.13	−
80	−	0	−	I_h	−0.06	−

[a] Up to the 36 H level the description is with respect to the hydrogenated carbon atoms. Above the 16 H level it is with respect to benzenoid rings and the hydrogen-free C_2 bond atoms. [b] See Figure 1 for numbering. [c] Symmetry of $C_{80}H_x$ molecule. [d] HBE per H_2 added to C_{80}, HBE/n = $\Delta E/n$, $n = x/2$; ΔE = reaction energy for $C_{80} + nH_2 \rightarrow C_{80}H_{2n}$. [e] HBE per H_2 added to *i*-Sc_3NC_{80}, HBE/n = $\Delta E/n$, $n = x/2$; ΔE = reaction energy for *i*-$Sc_3NC_{80} + nH_2 \rightarrow$ *i*-$Sc_3NC_{80}H_{2n}$. [f] 3−8, 13−16, 20, 21, 25−31, 35, 36, 40−42, 48, 49, 56, 57, 62, 73,76, 80.

with this isomer in order to underscore the subsequent calculations on I_h-*i*-Sc_3NC_{80}. Because of the difficulty accompanying calculations for large highly polyfluorinated fullerenes, for the incarcerated Sc_3N derivatives we have used the isostructural hydrogenated species as models cf. ref 18.

2. Computational Details

All calculations employed the DFT methodology with the ADF set of programs.[19] We used the local spin density approximation characterized by the electron gas exchange (Xα with $\alpha = 2/3$) together with the Vosko−Wilk−Nusair (VMN) parametrization[20] for correlation. Becke[21] and Perdew[22] nonlocal corrections were added to the exchange and correlation energy, respectively. Double-ζ+ polarization Slater basis sets were employed to describe the valence electrons of H, C, and triple-ζ+ polarization Slater basis sets for N and Sc. A frozen core composed of the 1s shell was described by means of single Slater functions for C and N, and 1s/2sp shells for Sc. The 3s and 3p electrons were described by double -ζ Slater functions, and the *n*d and (n + 1)s electrons by triple-ζ functions and the (n + 1)p electrons by a single orbital.[23] All energies are in eV.

3. Prediction of Addition Levels in C_{80} and *i*-Sc_3NC_{80}

3.1. Hydrogenation Binding Energies (HBE) for $C_{80}H_x$. As a first step we determined the most stable structures for compounds $C_{80}H_x$ (x = 2, 4, 16, 36, 44, 48, 52, 72, 76, 78, 80), thereby covering low (x = 2, 4), intermediate (x = 16, 36, 44, 48, 52), and high (x = 72, 76, 78, 80) addition levels. Each group has a particular rule for their stabilization. To obtain indications as to the most stable of them, a large number of isomers (including nonsymmetric structures) have been examined previously with the AIMPRO self-consistent density functional code running at the local spin density approximation (LSDA) level; this allows an economic calculation as a first step.[24] With AIMPRO we found that nonsymmetric structures for some stoicheiometries are isoenergetic compared with the analogous symmetric structures presented in Table 1. Some of the structures reported here could eventually be saddle points corresponding to hydrogen transfer between two minima. [Characterization would require the calculation of the vibrational frequencies, a huge computational effort.] The description of the most stable isomers of each stoicheiometry is given in Table 1, which shows the aromatic benzenoid rings, C=C bonds, symmetry, and the hydrogenation binding energies for the process $C_{80} + nH_2 \rightarrow C_{80}H_{2n}$. Specifically, we computed the HBE per added H_2 (referred to as HBE/n) above the C_{80} surface because this binding energy allows us to compare all stoicheiometries with each other. There are several possibilities for the first addition to the C_{80} surface, but we can expect the most pyramidalized 6:5 C_7-C_{23} bond ($\theta = 10.67°$)[25] which has the highest Mayer bond order (1.264) to be the most reactive site, HBE = −1.25 eV; for C_{80} numbering see Figure 1.

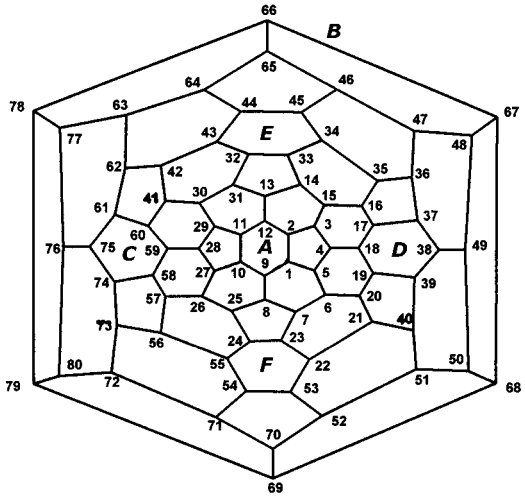

Figure 1. Schlegel diagram for C_{80} showing numbering. The capital letters represent the position of the benzenoid rings.

The product of H_2 addition across the C_1-C_9 6:6 bond is 0.61 eV less stable. Formation of $C_{80}H_4$ is predicted to involve addition of H_2 to C_1-C_2 followed by addition to the C_7-C_{23} 6:5 bond. By contrast, addition to the opposed remote $C_{78}-C_{79}$ or neighboring C_4-C_5 6:5 bonds gives isomers that are less stable by 0.38 and 1.20 eV, respectively. This suggests that it is profitable to investigate additions fairly near to C−C bonds that have already undergone addition. The most stable isomers of $C_{80}H_x$ (x = 16, 36, 44, 48, 52) involve hydrogen addition so as to produce aromatic (benzenoid) rings, as is the case in the formation of $C_{60}X_{18,36}$ (x = H, F).[26−28] $C_{80}H_{16}$ has only one benzenoid ring (A), whereas $C_{80}H_{44}$ has the maximum number of six (A−F). The latter structure adopts a 'cubic' shape due to the six planar aromatic faces together connected with twenty-two hydrogenated C−C bonds (see Figure 2a,b). $C_{80}H_{48}$ and $C_{80}H_{52}$ add the additional H_2 units to the E and F rings of $C_{80}H_{44}$ and consequently retain four benzenoid rings.

In the higher stoicheiometries (x = 72, 76, 78), there are no benzenoid rings, and the remaining free 6:5 bonds are separated

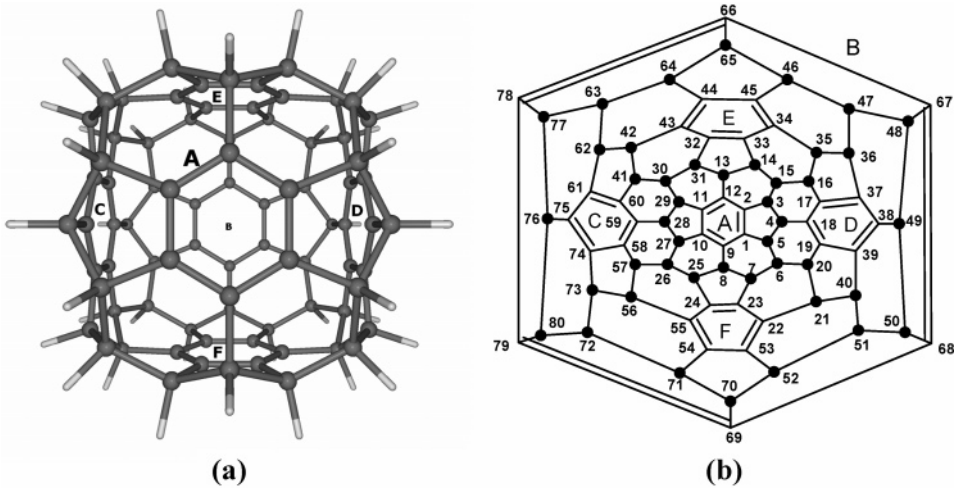

Figure 2. Optimized molecular structure (a) and Schlegel diagram (b, ● = H) for $C_{80}H_{44}$; the benzenoid rings are located in both for comparison.

as far possible from each other. Thus the two unhydrogenated C═C bonds in $C_{80}H_{76}$ are located in the opposite hemispheres at C_1-C_2 and $C_{78}-C_{79}$. Location of the sole unhydrogenated bond in $C_{80}H_{78}$ across a 6:5 bond (C_1-C_2) is marginally (0.11 eV) favored over a 6:6 bond (C_1-C_9). Full sphericity is restored in $C_{80}H_{80}$, the cage radius being 4.502 Å compared to 4.103 for C_{80}, due to C−C bond lengthening arising from strong H−H steric repulsions rather than to rehybridization effects.[29]

We have also analyzed the bonding between the C_{80} cage and the H_2 units using the extended transition method developed by Ziegler and Rouk[30] (an extension of the decomposition scheme of Morokuma).[31] According to this method, the binding energy (BE) between two fragments can be dissected into two main contributions:

$$\mathrm{BE} = (\Delta E_{\mathrm{DE}} + \Delta E_{\mathrm{INT}})$$

ΔE_{DE}, the deformation energy term, is the energy necessary to convert fragments from their equilibrium geometries to the cluster geometries. In our specific case, this comprises only the deformation energy of C_{80}, i.e. the energy difference between the free C_{80} and C_{80} with the geometry of the particular $C_{80}H_x$ compound. ΔE_{INT}, the interaction energy, represents the energy involved in the interaction between the deformed C_{80} fullerene and the nH_2 units. ΔE_{DE} is always > 0, i.e. destabilizing, whereas ΔE_{INT} can be > or < 0. An exothermic reaction requires $\Delta E_{\mathrm{INT}} < 0$ and $|\Delta E_{\mathrm{INT}}| > |\Delta E_{\mathrm{DE}}|$. Recently this method has been used very satisfactorily, to rationalize the ScN-cage bonding in *i*-Sc_3NC_k (k = 78, 80),[8] and the metal−C_{60} bonding in organometallic derivatives of C_{60}.[32] The components of the HBE values are collated in Table 2.

There is a relatively small variation in the HBE/n values between $C_{80}H_2$ and $C_{80}H_{44}$ (−1.25 and −1.08 eV per added H_2, respectively), but at higher hydrogenation levels the stabilities rapidly decrease, and $C_{80}H_{80}$ is only marginally stabilized (−0.06 eV per added H_2). This trend can be clearly seen in Figure 3 (circles). A parallel observation was found for C_{60} and C_{70} in that hydrogenation and fluorination led to maximum addend levels only of ca. 52 and 56, respectively.[33,34] A significant feature is that $C_{80}H_{44}$ possesses six benzenoid rings, the aromaticity of the latter arising from the presence of three sp^3 hybridized carbons in the two pentagons adjacent to each, thereby allowing delocalization without strain.[35]

From $C_{80}H_2$ to $C_{80}H_{52}$ the ΔE_{DE} values increase gradually from 1.40 to 1.62 eV but thereafter reduce substantially to 1.01 eV for $C_{80}H_{80}$. This trend is closely related to the deformation of the cage; at hydrogenation levels above $C_{80}H_{52}$ the C_{80} geometry becomes increasingly spherical again up to $C_{80}H_{80}$. The ΔE_{INT} values also increase slightly up to $C_{80}H_{44}$ but thereafter decrease even more rapidly than the ΔE_{DE} values due to the lack of reactivity of the remaining C═C bonds toward

TABLE 2: Deformation (ΔE_{DE}) and Interaction Energy (ΔE_{INT}) Components of the Hydrogenation Binding Energies per Added H_2 (HBE/n) for the Most Stable Isomers of $C_{80}H_x$

x	$\Delta E_{\mathrm{DE}}/n^a$	$\Delta E_{\mathrm{INT}}/n^b$	HBE/n^c
2	1.40	−2.65	−1.25
4	1.42	−2.66	−1.24
16	1.67	−2.71	−1.04
36	1.59	−2.64	−1.05
44	1.60	−2.68	−1.08
48	1.62	−2.54	−0.92
52:**1**	1.62	−2.45	−0.83
52:**5**	1.59	−2.41	−0.82
72	1.31	−1.66	−0.35
76	1.16	−1.36	−0.20
78	1.08	−1.21	−0.13
80	1.01	−1.07	−0.06

[a] $\Delta E_{\mathrm{DE}}/n = [E(C_{80}$* geometry fixed at $C_{80}H_x) - E(C_{80}$ optimized)]/n. [b] $\Delta E_{\mathrm{INT}}/n = [E(C_{80}$* + $nH_2 \rightarrow C_{80}H_{2n})]/n$. [c] HBE/$n$ = $\Delta E_{\mathrm{DE}}/n$ + $\Delta E_{\mathrm{INT}}/n$.

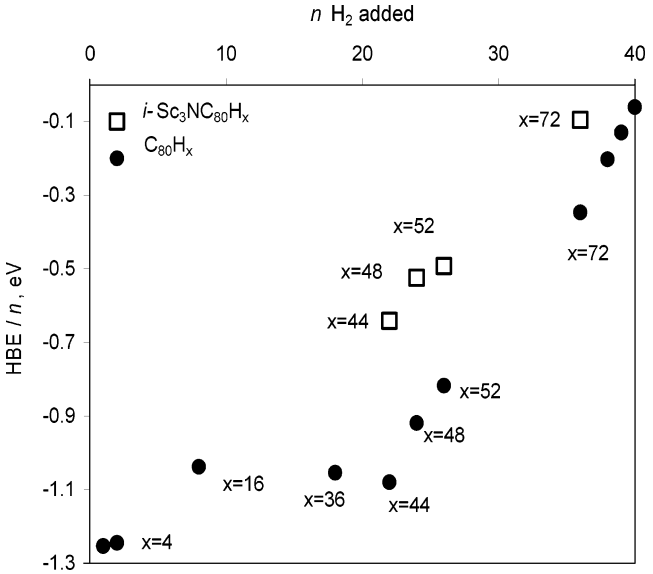

Figure 3. Hydrogenation Binding Energy per added H_2 (HBE/n) for series $C_{80}H_x$ (x = 2, 4, 16, 36, 44, 48, 52, 72, 76, 78 and 80), circles, and *i*-$Sc_3NC_{80}H_x$ (x = 44, 48, 52, 72), squares.

TABLE 3: Binding Energies (eV) for the Most Stable *i*-Sc_3NC_k and *i*-$Sc_3NC_{80}H_x$ Compounds

compound	isomer no.	ΔE_{DE}	ΔE_{INT}	HBE[a]	ΔE_{DE} Sc_3N	ΔE_{DE} cage	ΔE_{INT}	EBE[b]
i-Sc_3NC_{78}[c]	**1**	–	–	–	0.72	1.49	−11.91	−9.70
i-Sc_3NC_{80}[c]	**11**	–	–	–	0.79	0.58	−12.97	−11.6
i-$Sc_3NC_{80}H_{44}$	–	35.20	−58.96	−23.76	0.53	1.47	−5.69	−3.69
i-$Sc_3NC_{80}H_{48}$	–	38.95	−60.98	−22.03	0.57	1.84	−6.34	−3.93
i-$Sc_3NC_{80}H_{52}$	**5**	41.29	−62.56	−21.27	0.28	2.62	−7.83	−4.93
i-$Sc_3NC_{80}H_{72}$	–	47.09	−59.65	−12.56	0.34	2.55	−7.09	−4.21

[a] Hydrogenation binding energies for the reaction $C_{80} + nH_2 \rightarrow C_{80}H_{2n}$; HBE = $\Delta E_{DE} + \Delta E_{INT}$. [b] Encapsulation binding energies for the reactions $C_k + Sc_3N \rightarrow$ *i*-Sc_3NC_k (k = 78, 80) and $C_{80}H_x + Sc_3N \rightarrow$ *i*-$Sc_3NC_{80}H_x$ (x = 44,48,52,72); EBE = $\Delta E_{DE} + \Delta E_{INT}$. [c] From ref 8.

H_2. The C−C bonds at high $C_{80}H_x$ stoicheiometries are long and have low π-bond character. This seems to be the important factor in determining the notable change in HBE/n values at around $C_{80}H_{44}/C_{80}H_{52}$ stoicheiometry (Figure 3). For this reason, the $C_{80}H_{52}$ stoicheiometry is particularly important, and in the next section we focus on the encapsulation of Sc_3N nitride in several isomers of $C_{80}H_{52}$ in order to find the most stable one. Tables 1 and 2 present only a brief summary of the $C_{80}H_{52}$ study: the values for the most stable empty cage $C_{80}H_{52}$:**1**, and for the empty $C_{80}H_{52}$:**5** cage that produces the most stable *i*-$Sc_3NC_{80}H_{52}$:**5** compound.

3.2. Hydrogenation Binding Energies (HBE) for *i*-Sc_3NC_{80}. Cages $C_{80}H_x$ (x = 44, 48, 52, 72) selected for encapsulation with Sc_3N are completely deformed, consequently there is only one possible position where the nitride can be stabilized (see below). The nitride is planar in *i*-Sc_3NC_k (k = 68, 78, 80), but is pyramidal in most *i*-$Sc_3NC_{80}H_{52}$ studied isomers and *i*-$Sc_3NC_{80}H_{72}$ as it is a free molecule. We compare HBE/n for $C_{80}H_{2n}$ and *i*-$Sc_3NC_{80}H_{2n}$ to determine the difference in the values arising from adding H_2 units to the corresponding parents (last two columns of Table 1). The data for the *incar* compounds parallel those for the empty cages, except that the binding energy disadvantage on going to higher addition levels is even larger (see squares compared to circles in Figure 3). For example, the addition of 22 H_2 to empty C_{80} produces an energy of ca. 1.08 per added H_2, whereas the same addition to *i*-Sc_3NC_{80} gives an energy of only 0.64 eV per added H_2. Encapsulation of Sc_3N is a strongly exothermic process that is accompanied by a formal transfer of six electrons from the scandium to the fullerene cage, thereby making hydrogen addition less favorable. In large stoicheiometries such as *i*-$Sc_3NC_{80}H_{72}$ the lack of reactivity of the remaining C−C bonds also disfavors addition, and the HBE/n value is reduced to only −0.10 eV.

3.3. Sc_3N Encapsulation in Parent vs Hydrogenated Fullerenes. The comparison (Table 3) between *i*-Sc_3NC_k (k = 78, 80) and *i*-$Sc_3NC_{80}H_x$ (x = 44, 48, 52, 72) provides a measure of the energy involved in the encapsulation and hydrogenation processes.

The encapsulation binding energy (EBE) for $C_k + Sc_3N \rightarrow$ *i*-Sc_3NC_k is computed as −11.60 and −9.70 eV for k = 80 and 78, respectively. The deformation energy component (ΔE_{DE}) of EBE comprises the deformation produced in the Sc_3N nitride and the cage, both of which are small components, e.g. 1.37 eV in total for k = 80. The much more significant contributor to the EBE is the favorable interaction energy (ΔE_{INT}) arising from the electron transfer from nitride to fullerene cage and which for x = 80 is −12.97 eV. Whereas for *i*-Sc_3NC_k compounds only computation of encapsulation is required, *i*-$Sc_3NC_{80}H_x$ requires computation of both encapsulation and hydrogenation, for which two sequences exist. To simplify the calculations involved in finding the most stable structures of *i*-$Sc_3NC_{80}H_x$, we first narrow down the hydrogenated possibilities (in order to make the computations manageable) and then determine energies for placing Sc_3N inside them. Note that this simplification is based on the difference of the absolute EBE and HBE values. HBE values for $C_{80}H_x$ (x = 44, 48, 52) are ca. −22 eV, almost double the EBE involved in formation of *i*-Sc_3NC_{80} (−11.6 eV). Consequently, hydrogenation rather than encapsulation will determine the selection of the most stable isomers, so that this energy difference validates our procedure.

The HBE for $C_{80}H_x$ are dominated by the favorable ΔE_{INT} between the cages and the H_2 units and decrease in the order $C_{80}H_{44} > C_{80}H_{48} > C_{80}H_{52} > C_{80}H_{72}$. The EBE in these hydrogenated cages decrease drastically from −11.6 for *i*-Sc_3NC_{80} to ca. −4 for *i*-$Sc_3NC_{80}H_x$ (x = 44, 48, 52, 72) compounds due to an increase of ΔE_{DE} of the fullerene cage, but above all due to a decrease of the ΔE_{INT} between the hydrogenated cage and the nitride, i.e. −12.97 eV for *i*-Sc_3NC_{80} compared to ca. −7 for *i*-$Sc_3NC_{80}H_x$ (x = 44, 48, 52, 72) compounds. This less-effective interaction may reflect electron transfer from the nitride to the hydrogenated cage being less facilitated due to the lower acceptor character of the unoccupied orbitals of the hydrogenated cage compared to those of C_{80}. The decrease in the in-cage space and consequent increase in steric repulsion between the nitride and cage is involved in the ΔE_{INT} diminution.

The highest HBE is found in $C_{80}H_{44}$ and the highest EBE in *i*-$Sc_3NC_{80}H_{52}$:**5**. The EBE is favored by having a suitable in-cage space to incarcerate Sc_3N, the largest space being found in *i*-$Sc_3NC_{80}H_{52}$ among *i*-$Sc_3NC_{80}H_x$ (x = 44, 48, 52, 72). Note that the only marginally stabilized H_2 addition to *i*-Sc_3NC_{80} at higher addition levels is caused by HBE rather than EBE, as exemplified by *i*-$Sc_3NC_{80}H_{72}$ (−0.10 eV). Compared to *i*-$Sc_3NC_{80}H_{44}$ the HBE decreases from −23.76 to −12.56 eV, whereas the EBE are closely similar (−3.69 and −4.21 eV respectively).

4. Stabilities of Compounds $C_{80}H_{52}$, $C_{80}F_{52}$ and *i*-$Sc_3NC_{80}H_{52}$

A common experimental occurrence of a 52-addend level for hydrogenation and fluorination of *i*-Sc_3NC_{80} prompted a deeper investigation to find the most stable isomers of $C_{80}H_{52}$, $C_{80}F_{52}$, and *i*-$Sc_3NC_{80}H_{52}$ and the stabilizing factors affecting their relative energies. Following the procedure in section 3.3, the most stable structures obtained from hydrogenation were determined and then Sc_3N was encapsulated.

4.1. $C_{80}H_{52}$ and $C_{80}F_{52}$ Isomers. Fourteen isomers of $C_{80}H_{52}$ are collated in Table 4 showing the number of benzenoid rings, C═C bonds, and relative energies. Isomers **1**−**8** are the most stable, the stabilities differing by only 0.35 eV overall, with **1** being the most stable. These isomers uniquely each possess four benzenoid rings (A, B, C, D) and two C═C bonds in hexagons E and F, i.e. on opposite sides of the cage (see Figure 1 and Table 4). Isomers **9** and **10** also have four benzenoid rings, but here the C═C bonds are not located in hexagons **E** and **F** and this is seen to have a marked difference on the calculated stabilities. The calculated energies for isomers **9**−**14** are also high due evidently to the lower number of benzenoid rings in the structures, and thus the least stable isomers **13** and **14** have no benzenoid rings, the 14 C═C bonds being spread around the cage.

The Schlegel diagram and optimized structure of $C_{80}H_{52}$:**1** are shown in Figure 4. The lengths of the C−C bond in the aromatic benzenoid rings are calculated to vary only from 1.377 to 1.386 Å, the aromaticity being confirmed also by the

TABLE 4: Description and Relative Energies (*R*) of $C_{80}H_{52}$, $C_{80}F_{52}$, and *i*-$Sc_3NC_{80}H_{52}$ Isomers[a]

isomer no.	benzenoid rings[b]	C═C bond[c]	sym[d]	*R*(eV) $C_{80}H_{52}$	*R*(eV) $C_{80}F_{52}$	*R* (eV) i-$Sc_3NC_{80}H_{52}$
1	A,B,C,D	23,24;32,33	C_{2v}	0.00	0.00	0.00
2	A,B,C,D	23,24;44,45	C_{2h}	0.03	0.05	−0.39
3	A,B,C,D	22,53;32,33	C_1	0.18	−	−
4	A,B,C,D	22,23;32,33	C_2	0.32	0.51	0.43
5	A,B,C,D	22,23;33,34	C_s	0.31	0.50	−0.55
6	A,B,C,D	22,23;32,43	C_2	0.35	0.55	−0.25
7	A,B,C,D	22,23;34,45	C_2	0.32	0.51	0.44
8	A,B,C,D	22,23;44,45	C_i	0.35	0.58	−
9	A,B,C,D	7,23;14,33	C_s	1.73	2.21	1.77
10	A,B,C,D	21,22;42,43	C_2	2.26	3.07	−
11	A,B	17,37;19,39;22,23; 24,55;32,43;33,34; 58,74;60,61	C_s	1.39	0.19	−
12	A,B	17,18;22,23;24,55; 32,43;33,34;38,39; 58,59;61,75	C_2	1.44	0.79	0.49
13	−	*e*	C_s	5.24	5.22	−
14	−	*f*	C_{2v}	3.58	4.04	2.90

[a] Description with respect to hydrogen-free carbons, benzenoid rings, and C_2 free bonds. [b] See Figure 1. [c] Double bond locations, either 6:6 or 6:5 bonds. [d] Symmetry of $C_{80}H_{52}$ and $C_{80}F_{52}$ isomers. [e] 1,5;7,23;10,27;14,33;17,37;19,39;31,32;44,64;45,46;50,68;52,53;58,74,60;61;79,80. [f] 4,18; 8,9;12,13;22,23;24,55;28,59;32,43;33,34;36,47;40,51;62,63;65,66;69,70;72,73.

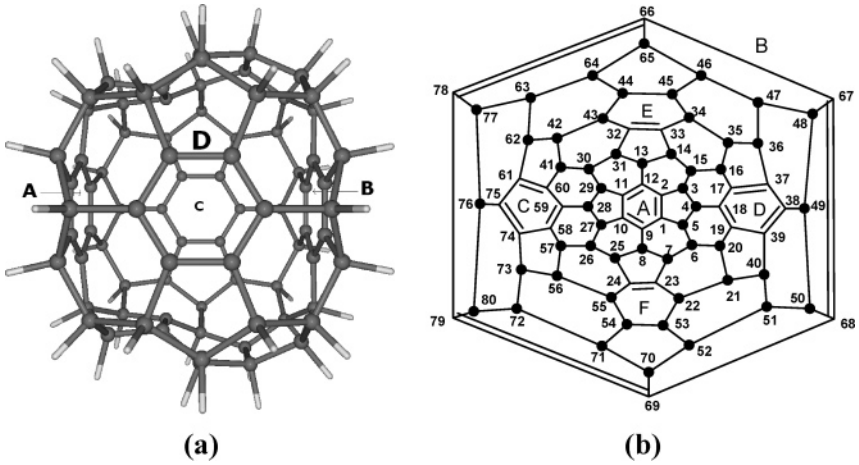

Figure 4. Optimized molecular structure (a) and the Schlegel diagram (b, ● = H) for $C_{80}H_{52}$:**1**. Structure (a) is rotated relative to the Schlegel diagram. The benzenoid rings are located in both for comparison.

calculated planarity. This parallels the structural situation found experimentally for $C_{60}H_{36}$ isomers.[27] The lengths of the isolated C═C bonds are calculated as 1.335 Å. The resultant structure resembles a cube with four planar faces and two wrinkled ones which contain the C═C bonds, and notably, the hydrogenation of 26 C−C bonds in C_{80} produces a major distortion of the original shape. The C−C bond lengths for the other isomers differ little from the above values.

Results for fluorination are similar, except that isomer **11** is relatively more stable than the hydrogenated counterpart. The C−F distances for the most stable isomer **1** are calculated to range from 1.367 to 1.396 Å which parallels the values found for $C_{60}F_{48}$ (1.362−1.395 Å)[36] and $C_{60}F_{18}$ (1.361−1.396 Å).[37] This indicates that the present level of computing is very satisfactory. The similar results for H and F atoms allow us to use, with some confidence, hydrogen as a model for calculating the energies of the *incar* Sc_3N derivatives.

4.2. *i*-$Sc_3NC_{80}H_{52}$ Isomers. To construct the *i*-$Sc_3NC_{80}H_{52}$ isomers we encapsulated the Sc_3N unit retaining some symmetry properties such as symmetry plane or C_2 axis and also orientating the Sc atoms over the C═C bonds and the benzenoid rings. These requirements and the space limitation of the fullerene restrict the stabilizing orientation of the nitride in each $C_{80}H_{52}$ isomer to one possibility only. By contrast, in *i*-Sc_3NC_{80} the Sc_3N unit is not trapped in a specific position and free rotation is expected.[8] The preference for Sc atoms to be close to the free C atoms is expected because the latter can use their p_z orbitals to make Sc−C bonds. Moreover, to accomplish these requirements, Sc_3N adopts a pyramidal structure in most of the isomers.

Isomers of *i*-$Sc_3NC_{80}H_{52}$ were optimized from $C_{80}H_{52}$ isomers **1**, **2**, **4**−**7**, **9** that have four benzenoid rings, and also isomers **12** and **14** that have two and no benzenoid rings, respectively; lack of symmetry precluded calculations on isomers **3**, **8**, **10**, and **11**. The relative energies show significant differences from those of their empty-cage counterparts (see last column, Table 4), but the most stable *i*-$Sc_3NC_{80}H_{52}$ isomers come from the first eight most stable $C_{80}H_{52}$ isomers. Isomers *i*-$Sc_3NC_{80}H_{52}$: **2**, **5**, and **6** are predicted to be more stable than isomer *i*-$Sc_3NC_{80}H_{52}$:**1** (derived from the most stable $C_{80}H_{52}$ isomer) with *i*-$Sc_3NC_{80}H_{52}$:**5** the most stable overall; both isomers are displayed in Figures 5 and 6.

The substantial alteration of the relative energies as a result of encapsulation of Sc_3N arises from different interaction between the nitride and the relevant hydrogenated cage, together with the different number and strength of the Sc−C bonds. This argument is developed further in section 4.3. The geometric and electronic structure of the most stable isomer *i*-$Sc_3NC_{80}H_{52}$:**5**

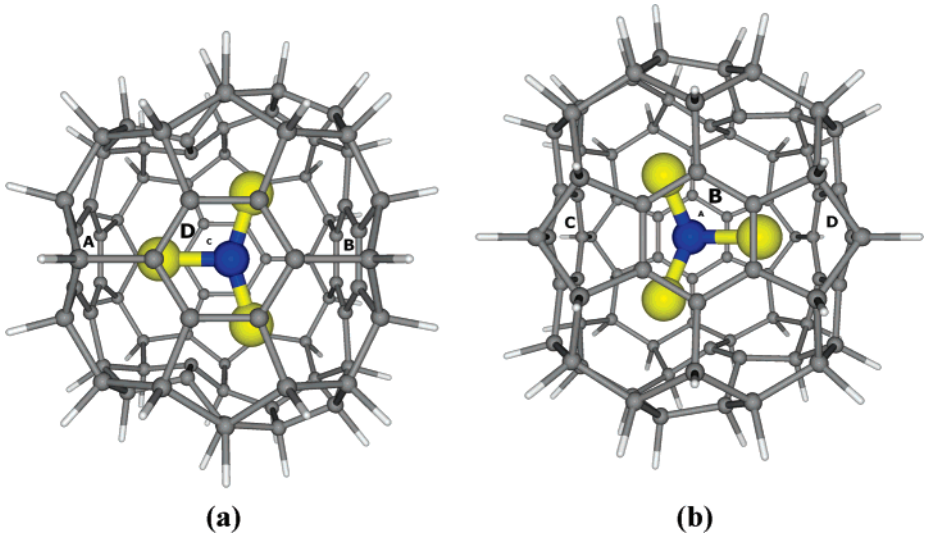

Figure 5. Optimized molecular structures of (a) *i*-$Sc_3NC_{80}H_{52}$:**1** and (b) *i*-$Sc_3NC_{80}H_{52}$:**5**; the benzenoid rings are located in each picture.

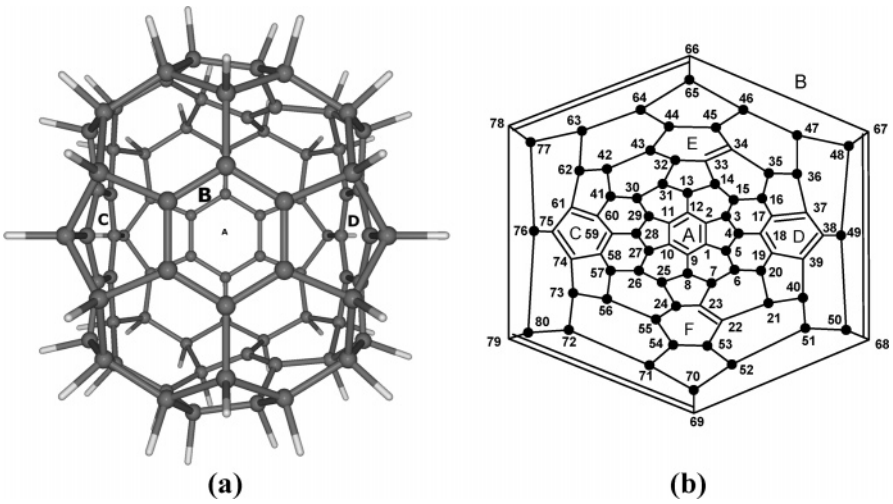

Figure 6. Optimized molecular structure (a) and Schlegel diagram (b, ● = H) for $C_{80}H_{52}$:**5**; the benzenoid rings are located in both for comparison.

is considered first, followed by determination of the factors that affect the stabilization of the *i*-$Sc_3NC_{80}H_{52}$ isomers.

4.3. Geometric and Electronic Structure of *i*-$Sc_3NC_{80}H_{52}$: 5. Some values (eV, same computational level) of the HOMO−LUMO gap (a measure of stability) are: I_h-C_{80}, 2.23; $C_{80}H_{52}$:**5**, 3.96; *i*-Sc_3NC_{80}:**11**, 1.18; *i*-$Sc_3NC_{80}H_{52}$:**5**, 0.23. The latter thus appears to be the least stable among this family of compounds. When Sc_3N is encapsulated by $C_{80}H_{52}$:**5**, there is significant local distortion in the hydrogenated cage. In this isomer, two Sc atoms face the two isolated C═C bonds (C_{22}−C_{23} and C_{33}−C_{34}) and the other faces benzenoid ring D and two atoms of B (see Figure 5b). This distortion results in inward movement of the non-hydrogenated carbon atoms until they attain bonding Sc−C distances. The benzenoid ring B is moved substantially inward. The pyramidal Sc_3N unit (Sc−N distance of 1.921 Å, cf. 1.957 Å in the free molecule (see Table 5)), is unable to either rotate or fluctuate; i.e. it is completely fixed in this orientation. The cage otherwise retains the overall structure of the $C_{80}H_{52}$:**5** precursor (Figure 6). Hence hydrogenation determines the main geometric features of the cage, while encapsulation produces modification.

During the geometrical optimization process, the contacts between Sc and free C atoms become favored and maximized. The average distance between Sc and the eight carbons of benzenoid ring D and two of ring B decrease to a bonding distance of 2.391 Å. The aromaticity of these two rings is broken and the range of C−C distances within them is increased (1.384−1.446 Å). The other nonbonded benzenoid rings (A and C) retain their aromaticity. The shortest Sc−C distances (2.293 Å) are found between the other two Sc atoms and one of the carbon atoms of the two C═C bonds. Due to these $Sc-C_2$ bonds, the C═C bond lengths of the cage are increased by 0.085 Å. These Sc−C distances fall within the range of values obtained in an exploration of 73 examples in the Cambridge Structural Database, where the mean is 2.430 Å and the shortest 2.204 Å.

TABLE 5: Optimized Distances (Å) for *i*-$Sc_3NC_{80}H_{52}$ Isomers

isomer no.	average N−Sc distance[a]	no. of $Sc-C_2$ connections	mean Sc−C distance[b]	no. of $Sc-C_6$ connections	mean Sc−C distances
1	1.879	4	2.224	6	2.361
2	1.895	4	2.326	6	2.387
4	1.884	4	2.391	6	2.366
5	1.921	4	2.423	8	2.391
6	1.897	4	2.313	6	2.437
7	1.891	4	2.363	6	2.371
9	1.903	2	2.269	8	2.388
12	1.877	6	2.318	–	
14	1.920	4	2.364	–	

[a] Calculated as 1.957 Å in Sc_3N. [b] Calculated as 2.276 Å in *i*-Sc_3NC_{80}.

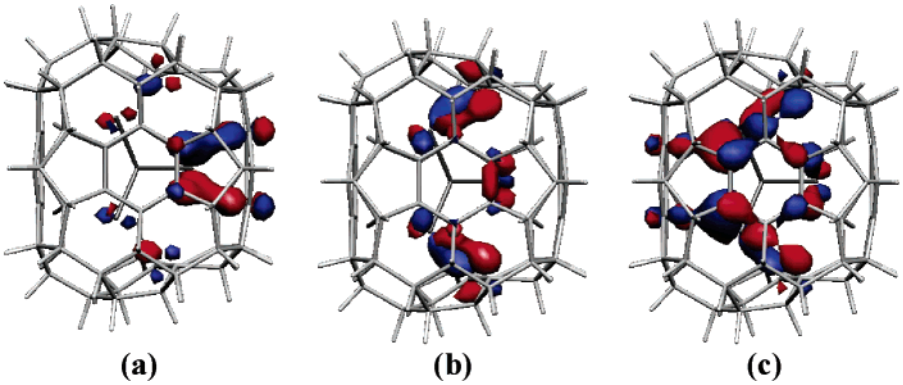

Figure 7. The three highest occupied molecular orbitals of *i*-$Sc_3NC_{80}H_{52}$:**5**. The orbitals represent the bonding between (a) Sc atom and the 6 carbon atoms of the D benzenoid ring, (b) two Sc atoms and the two C=C bonds ($C_{22}-C_{23}$, $C_{33}-C_{34}$), and (c) Sc atom and the B benzenoid ring. All orbitals comprise the empty Sc d-orbitals and π^* C−C orbitals of $C_{80}H_{52}$:**5**.

TABLE 6: Relative[a] and Binding Energies[a] (eV) for the Most Stable *i*-$Sc_3NC_{80}H_{52}$ Isomers

						ΔE_{DE}					
isomer no.	sym[b]	ΔE_{DE}	ΔE_{INT}	HBE[b]	relative HBE	Sc_3N	cage	ΔE_{INT}	EBE[c]	relative EBE	total relative energy[d]
1	C_s	42.02	−63.58	−21.56	0.00	0.56	2.31	−6.94	−4.07	0.00	0.00
2	C_2	42.04	−63.57	−21.53	0.03	0.49	2.64	−7.62	−4.49	−0.42	−0.39
4	C_2	41.41	−62.64	−21.23	0.33	0.56	2.59	−7.12	−3.97	0.10	0.43
5	C_s	41.30	−62.55	−21.25	0.31	0.28	2.62	−7.83	−4.93	−0.86	−0.55
6	C_2	41.12	−62.33	−21.21	0.35	0.48	2.62	−7.77	−4.67	−0.60	−0.25
7	C_2	41.41	−62.65	−21.24	0.32	0.54	2.49	−6.98	−3.95	0.12	0.44
9	C_s	–	–	−19.83	1.73	–	–	–	−4.03	0.04	1.77
12	C_2	–	–	−20.12	1.44	–	–	–	−5.02	−0.95	0.49
14	C_{2v}	–	–	−17.98	3.58	–	–	–	−4.75	−0.68	2.90

[a] The relative energies of *i*-$Sc_3NC_{80}H_{52}$ isomers comprise the energy required to hydrogenate C_{80} to the $C_{80}H_x$ isomers (HBE) and the energy of incarcerating Sc_3N (EBE). This necessarily differs from the experimental sequence involving encapsulation followed by hydrogenation. [b] Symmetry of *i*-$Sc_3NC_{80}H_{52}$ which in some cases is reduced from corresponding $C_{80}H_{52}$ isomers. [c] Hydrogenation binding energy (HBE), ΔE for $C_{80} + 26\ H_2 \rightarrow C_{80}H_{52}$. HBE = $\Delta E_{DE} + \Delta E_{INT}$. [c] Encapsulation binding energy (EBE), ΔE for $C_{80}H_{52} + Sc_3N \rightarrow$ *i*-$Sc_3NC_{80}H_{52}$. EBE = $\Delta E_{DE} + \Delta E_{INT}$. ΔE_{DE} = ΔE_{DE} (Sc_3N) + ΔE_{DE} (cage). [d] Total relative energy = relative HBE + relative EBE.

Both experimental (2.170 Å) and theoretical (2.276 Å) distances for *i*-Sc_3NC_{80}[8] were shorter than the calculated Sc−C distances in *i*-$Sc_3NC_{80}H_{52}$:**5**. The presence of bonding Sc−C distances and the potential for trapping of Sc_3N in a specific position prompted us to investigate the possibility of strong Sc−C bonds between the Sc_3N unit and the hydrogenated cage.

However, *i*-Sc_3NC_{80} may be *formally* described by the ionic model *i*-$[Sc_3N]^{6+}[C_{80}]^{6-}$ involving the transfer of six electrons from the three highest occupied nitride orbitals to the three lowest unoccupied orbitals of C_{80} and free rotation of Sc_3N unit. The electronic structure of *i*-$Sc_3NC_{80}H_{52}$:**5** is characterized not only by the ionic interaction but also by orbital interactions of both fragments which incarcerate the Sc_3N in a specific position. Likewise, there is formal transfer of six electrons from the three highest occupied orbitals of Sc_3N unit to the three lowest unoccupied orbitals of $C_{80}H_{52}$ molecule, which become the three HOMOs of the new *i*-$Sc_3NC_{80}H_{52}$:**5** complex. These cage orbitals, which represent π^* C−C orbitals of $C_{80}H_{52}$:**5** also become highly stabilized due to bonding interactions with empty d metal orbitals, so explaining the strong link between Sc atoms and the free C atoms of the cage. The three bonding orbitals are displayed in Figure 7.

4.4. Factors Affecting the Stabilization Energies. The relative energies were analyzed in terms of their components in order to determine the origin of the differences among the *i*-Sc_3NC_{80} isomers (Table 6). To aid this analysis, the N−Sc bond lengths and the different type of Sc-cage connections with their respective lengths are collated in Table 5. The main contributions to the relative energy (HBE and EBE) can each be dissected into the deformation energy (ΔE_{DE}) and the interaction energy (ΔE_{INT}). As seen from Table 6, EBE but not HBE is the crucial component of the relative energy and determines the stability order of the *i*-$Sc_3NC_{80}H_{52}$ isomers. Thus while *i*-$Sc_3NC_{80}H_{52}$:**5**, the most stable isomer, does not have the highest HBE, it has the highest EBE of −4.93 eV. For the first eight most stable $C_{80}H_{52}$ isomers the relative HBE ranges between 0.00 and 0.35 eV whereas the relative EBE between 0.44 and −0.55 eV. So the differences in the interaction between Sc_3N and the different $C_{80}H_{52}$ cages determine the final relative energy of *i*-$Sc_3NC_{80}H_{52}$ isomers. This isomer is therefore the most favorable because Sc_3N unit is encapsulated favoring Sc−C contacts, shown by the maximum interaction term (ΔE_{INT} = −7.83 eV) and minimum deformation of Sc_3N (ΔE_{DE} = 0.28 eV) compared to the other isomers.

Unlike isomers *i*-$Sc_3NC_{80}H_{52}$:**1**, **2**, **4**, **6**, and **7**, which have at least four Sc−C_2 type and six Sc−C_6 type interactions, the most stable isomer *i*-$Sc_3NC_{80}H_{52}$:**5** has the advantage of two additional Sc−C_6 type interactions. Moreover, these two additional bonding interactions are obtained with only minor distortion of the Sc_3N unit. Finally, it is noteworthy that for encapsulation of Sc_3N unit inside isomers $C_{80}H_{52}$:**12** and **14** the EBE is not enough to counteract the destabilization produced by the HBE. This is important because it deters searching for *i*-$Sc_3NC_{80}H_{52}$ with a HBE of C_{80} destabilized more than 1 eV (the highest relative EBE found has been −0.95 eV for $Sc_3NC_{80}H_{52}$:**12**).

In conclusion, the most stable *i*-$Sc_3NC_{80}H_{52}$ isomer is that in which the Sc_3N unit can be hosted to allow the highest number of bonding interactions between the Sc atoms and the 28 free carbon atoms, provided the destabilization produced by the HBE is not too high. This has allowed us to predict the most stable isomers for *i*-$Sc_3NC_{80}H_x$ (x = 44, 48, 72) compounds.

Acknowledgment. We thank MCYT of the Government of Spain and the CIRIT of the Catalan government (Grants no. BQU2002−04110−C02-02 and SGR01-00315) for financial support. J.M.C. thanks Agència de Gestió d'Ajuts Universitaris i de Recerca (AGAUR) of the Generalitat de Catalunya for financial support during his visit to Sussex University.

References and Notes

(1) Stevenson, S.; Fowler, P. W.; Heine, T.; Duchamp, J. C.; Rice, G.; Glass, T.; Harich, K.; Hajdu, E.; Bible, R.; Dorn, H. C. *Nature* **2000**, *408*, 427.

(2) Olmstead, M. M.; de Bettencourt-Dias, A.; Duchamp, J. C.; Stevenson, S.; Marciu, D.; Dorn, H. C.; Balch, A. L. *Angew. Chem., Int. Ed.* **2001**, *40*, 1223.

(3) Olmstead, M. M.; de Bettencourt-Dias, A.; Duchamp, J. C.; Stevenson, S.; Dorn, H. C.; Balch, A. L. *J. Am. Chem. Soc*. **2000**, *122*, 12220.

(4) Lee, H. M.; Olmstead, M. M.; Iezzi, E. B.; Duchamp, J. C.; Dorn H. C.; Balch, A. L. *J. Am. Chem. Soc*. **2002**, *124*, 3494.

(5) Duchamp, J. C.; Demortier, A.; Fletcher, K. R.; Dorn, D.; Iezzi, E. B.; Glass, T.; Dorn, H. C. *Chem. Phys. Lett*. **2003**, *375*, 655.

(6) Stevenson, S.; Lee, H. M.; Olmstead, M. M.; Kozikowski, C.; Stevenson P.; Balch, A. L. *Chem. Eur. J*. **2002**, *8*, 4528.

(7) Fowler, P. W.; Zerbetto, F. *Chem. Phys. Lett.* **1995**, *243*, 36.

(8) Campanera, J. M.; Bo, C.; Olmstead, M. M.; Balch, A. L.; Poblet, J. M. *J. Phys. Chem. A* **2002**, *106*, 12356.

(9) Kobayashi, K.; Sano, Y.; Nagase, S. *J. Comput. Chem*. **2001**, *22*, 1353.

(10) Ioffe, I. N.; Ievlev, A. S.; Boltalina, O. V.; Sidorov, L. N.; Dorn, H. C.; Stevenson, S.; Rice, G. *Int. J. Mass Spectrom*. **2002**, *213*, 183.

(11) Stevenson, S.; Rice, G.; Glass, T.; Harich, K.; Cromer, F.; Jordan, M. R.; Hadju, E.; Bible, R.; Olmstead, M. M.; Maitra, K.; Fischer, A. J.; Balch, A. L.; Dorn, H. C. *Nature* **1999**, *401*, 55.

(12) Iezzi, E. B.; Duchamp, J. C.; Harich, K.; Glass, T.; Lee, H. M.; Olmstead, M. M.; Balch A. L.; Dorn, H. C. *J. Am. Chem. Soc*. **2002**, *124*, 524. Lee, H. M.; Olmstead, M. M.; Iezzi, E. B.; Duchamp, J. C.; Dorn, H. C.; Balch, A. L. *J. Am. Chem. Soc*. **2002**, *124*, 3494.

(13) Iezzi, E. B.; Cromer, F.; Stevenson P.; Dorn, H. C. *Synth. Metals* **2002**, *128*, 289.

(14) Darwish, A. D.; Dorn, H. C.; Taylor, R. unpublished work.

(15) Darwish, A. D.; Avent, A. G.; Boltalina, O. V.; Stevenson S.; Taylor, R., unpublished work.

(16) Hennrich, F. H.; Michel, R. H.; Fischer, A.; Richard-Schneider, S.; Gilb, S.; Kappes, M. M.; Fuchs, D.; Bürk, M.; Kobayashi, K.; Nagase, S. *Angew. Chem., Int. Ed. Engl.* **1996**, *35*, 1732.

(17) Wang, C.-R.; Sugai, T.; Kai, T.; Tomiyama, T.; Shinohara, H. *Chem. Commun.* **2000**, 557.

(18) Fowler, P. W.; Sandall, J. P. B.; Taylor, R. *J. Chem. Soc., Perkin Trans. 2* **1997**, 419.

(19) ADF 2000.01, SCM, Theoretical Chemistry, Vrije Universiteit, Amsterdam, The Netherlands, www.scm.com; Baerends, E. J.; Ellis, D. E.; Ros, P. *Chem. Phys*. **1973**, *2*, 41. Versluis, L.; Ziegler, T. *J. Chem. Phys*. **1988**, *332*, 88. te Velde, G.; Baerends, E. J.; *J. Comput. Phys*. **1992**, *99*, 84. Fonseca Guerra, C.; Snijders, J. G.; te Velde, G.; Baerends, E. J. *Theor. Chem. Acc.* **1998**, *99*, 391.

(20) Vosko, S. H.; Wilk, L.; Nusair, M. *Can. J. Phys*. **1980**, *58*, 1200.

(21) Becke, A. D. *J. Chem. Phys*. **1986**, *84*, 4524; *Phys. Rev*. **1988**, *A38*, 3098.

(22) Perdew, J. P. *Phys. Rev*. **1986**, *B34*, 7406.

(23) Snijders, J. G.; Baerends, E. J.; Vernooijs, P. *At. Nucl. Data Tables* **1982**, *26*, 483. Vernooijs, P.; Snijders, J. G.; Baerends, E. J. *Slater-type Basis Functions for the Whole Periodic System*; Internal Report, Vrije Universiteit, Amsterdam, The Netherlands, 1981.

(24) Jones, R.; Briddon, P. R. *Semicond. Semimet*. **1998**, *51A*, 287.

(25) Haddon, R. C.; Scott, L. T. *Pure Appl. Chem*. **1986**, *58*, 137; Haddon, R. C.; Chow, S. Y. *J. Am. Chem. Soc*. **1998**, *120*, 10494.

(26) Darwish, A. D.; Avent, A. G.; Taylor, R.; Walton, D. *J. Chem. Soc., Perkin Trans. 2*, **1996**, 2051. Boltalina, O. V.; Markov, V. Yu.; Taylor, R.; Waugh, M. P. *Chem. Commun*. **1996**, 2549. Boltalina, O. V.; Street, J. M.; Taylor, R. *J. Chem. Soc., Perkin Trans. 2* **1998**, 649.

(27) Hitchcock, P. B.; Taylor,R**.** *Chem. Commun*. **2002**, 2078. Avent, A. G.; Clare, B. W.; Hitchcock, P. B.; Kepert, D. L.; Taylor, R. *Chem. Commun*. **2002**, 2370.

(28) Nossal, J.; Saini, R. K.; Sadana, A. K.; Bettinger, H. F.; Alemany, L. B.; Scuseria, G. E.; Billups, W. E.; Saunders: M.; Khong, A.; Weisemann, R. *J. Am. Chem. Soc.* **2001**, *123*, 8482.

(29) Cioslowski, J. *Chem. Phys. Lett*. **1991**, *181*, 68.

(30) Ziegler, T.; Rauk, A. *Teor. Chim. Acta* **1977**, *46*, 1; *Inorg. Chem*. **1979**, *18*, 1558.

(31) Morokuma, K. *J. Chem. Phys*. **1971**, *55*, 1236. Kitaura, K.; Morokuma, K. *Int. J. Quantum Chem*. **1976**, *10*, 325.

(32) Nunzi, F.; Samellotti, A.; Re, N.; Florianai, C. *Organometallics* **2000**, *19*, 1628.

(33) For collation of data and leading references, see Taylor, R.; Langley, G. J.; Holloway, J. H.; Hope, E. G.; Brisdon, A. K.; Kroto, H. K.; Walton, D. R. M. *J. Chem. Soc., Perkin Trans. 2* **1995**, 181.

(34) Darwish, A. D.; Abdul-Sada, A. K.; Langley, G. J.; Kroto, H. W.; Taylor, R.; Walton, D. R. M. *J. Chem. Soc., Perkin Trans. 2* **1995**, 2359.

(35) Taylor, R. *Philos. Trans. R. Soc. London, A* **1993**, *343*, 87. Austin, S. J.; Batten, R. C.; Fowler, P. W.; Redmond, D. B.; Taylor, R. *J. Chem. Soc., Perkin Trans. 2* **1993**, 1383.

(36) Troyanov, S. I.; Troshin, P. A.; Boltalina, O. V.; Ioffe, I. N.; Sidorov, L. N.; Kemnitz, E. *Angew. Chem., Int. Ed.* **2001**, *40*, 2285.

(37) Neretin, I. S.; Lyssenko, K. A.; Antipin, M. Yu.; Slovokhotov, Yu. L.; Boltalina, O. V.; Troshin, P. A.; Lukonin, A. Yu.; Sidorov, L. N.; Taylor, R. *Angew. Chem., Int. Ed.* **2000**, *39*, 3273.